JOC The Journal of Organic Chemistry

Article

pubs.acs.org/joc

Decarboxylation without CO_2: Why Bicarbonate Forms Directly as Trichloroacetate Is Converted to Chloroform

Graeme W. Howe and Ronald Kluger*

Davenport Chemical Laboratories, Department of Chemistry, University of Toronto, 80 St. George Street, Toronto, Ontario M5S 3H6, Canada

Supporting Information

ABSTRACT: Patterns in the observed catalysis of decarboxylation reactions required us to conclude that these reactions involve initial hydration of the carboxylate and subsequent loss of bicarbonate. This raises the important and general question of why CO_2 is not formed directly. Reaction profiles for the direct decarboxylation of trichloroacetate were generated with DFT calculations and show no significant barrier to the recombination of the incipient trichloromethide and CO_2. In contrast, cleavage of the C−C bond from the hydrated intermediate shows a substantial barrier to recombination that allows separation of the products. The free energy of the transition state for C−C bond cleavage following hydration is higher than the free energy for formation of the hydrate and is comparable to the free energy of activation for direct decarboxylation. Thus, we conclude that the advantage of the hydrolytic pathway is that it provides a means to overcome the problems of separation and solvation that hinder the direct loss of CO_2. The resulting concepts are readily extended to explicating the mechanisms of processes in enzymic catalysis as well as providing a basis for producing C−C bonds by the addition of derivatives of carbanions to carbonates.

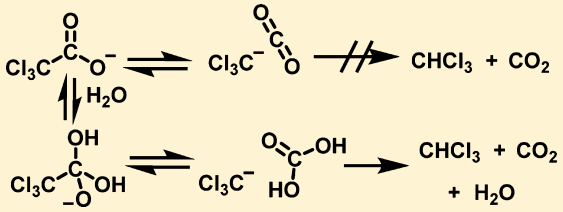

INTRODUCTION

Decarboxylations in water are typically considered to proceed as electrophilic substitution reactions through a single step in which C−C bond cleavage produces CO_2 along with a residual carbanion (Scheme 1).[1,2] However, the observation that the decarboxylation of mandelylthiamin is subject to general base catalysis is incompatible with a single-step decarboxylation mechanism.[3] Rather, that observation is consistent with initial addition of water to the carboxyl group, producing an intermediate from which transfer of a proton is concerted with C−C bond cleavage, releasing bicarbonate and the carbanion (Scheme 2). Similar hydrated intermediates have recently been proposed to account for observations of properties of certain enzyme-catalyzed decarboxylation reactions.[4,5] Since those pathways do not change the nature of the carbanionic product, formation of an alternative to CO_2 by hydration must be able to overcome problems that are inherent to the direct formation of CO_2. In particular, C−C cleavage from the hydrate in neutral solutions produces carbonic acid or bicarbonate. These are weaker electrophiles than CO_2 and are more readily solvated by water,[6−8] providing a potential energetic basis for the existence of those alternatives.

Scheme 1. Recombination Competes with Separation along the Dissociative Pathway for Decarboxylation

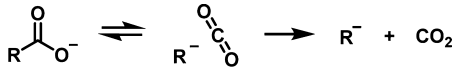

Scheme 2. Bond Cleavage following Hydration Gives Bicarbonate Instead of Carbon Dioxide

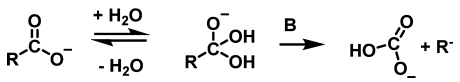

Several high-level computational analyses of decarboxylation reactions that produce localized carbanions and CO_2 have been reported.[9−14] Gao and Major[15] produced a free energy reaction profile for the decarboxylation of *N*-methyl picolinic acid. Lee and Houk[16] arrived at the enthalpic reaction profiles for the decarboxylation of orotidylic acid by several routes. These studies reveal that energy increases with C−C bond length, reaching a maximum with no significant decrease with increasing distance between CO_2 and the nascent carbanion. In principle, increasing entropy would become significant in such a system at realistic reaction temperatures. However, the essential similarities suggest that the lack of a significant barrier to the recombination of CO_2 and the nascent carbanion interferes with formation of the required products. In contrast, where the charge on the nascent carbanion is effectively depleted internally, as in the decarboxylation of 3-carboxybenzisoxazaoles,[17] the computed free energy profile exhibits a sharp drop in energy at distances beyond the initial maximum, thereby avoiding the problem of recombination.[18]

The decarboxylation of trichloroacetate (TCA) in water produces a localized trichloromethyl anion.[19] That anion is

Received: August 28, 2014
Published: October 23, 2014

ACS Publications © 2014 American Chemical Society

protonated by water to form chloroform in addition to CO_2. Interestingly, various reports over many years have indicated that the reaction is probably base-catalyzed.[20−22] However, base catalysis has no role in a pathway that forms CO_2 directly as there are no proton-transfers in the C−C cleavage step. Yet, based on the observed carbon kinetic isotope effect,[20] C−C cleavage does occur in the rate-determining step. Therefore, the acceleration by base suggests that the reaction is susceptible to a hydrolytic route.

Kresge and co-workers studied the base-catalyzed deprotonation of chloroform.[23] The reaction produces the trichloromethyl anion by transfer of a proton to Brønsted bases. The rate-limiting step in this system is the separation of products from proton-transfer. The decarboxylation of trichloroacetate generates the same carbanion as the deprotonation of chloroform. Unlike proton-transfer reactions, with CO_2 as the electrophilic leaving group, there is no acceptor for the electrophile that drives the reaction forward. Furthermore, the low solubility of CO_2 in aqueous solution[24,25] minimizes the extent to which solvation can assist the separation of the trichloromethyl anion and CO_2.

In the present study, we report our analysis by density functional theory (DFT) calculations of the pathways for decarboxylation of TCA. Reaction profiles generated with a wide range of levels of theory consistently indicate that no energetic minimum is reached by the direct loss of CO_2 from TCA. This implies that the recombination of the incipient carbanion and CO_2 is a barrier-free process. Reaction profiles from the proposed hydrated intermediate (as in Scheme 2) show a more pronounced barrier to the recombination. We also report calculations on the thermodynamics of carboxylate hydration, which is a precursor in the hydrolytic pathway. While formation of the hydrate is clearly endergonic, we find that the overall free energy of activation for the hydrolytic mechanism is nearly identical to that which would lead to the direct loss of CO_2 were it able to separate from the carbanion. The clear advantage of the hydrolytic mechanism is that carbon−carbon bond cleavage produces a less reactive and better solvated alternative to CO_2, overcoming the intrinsic problems of recombination of the reactive products.

COMPUTATIONAL METHODS

All calculations were carried out with Gaussian 09.[26] Throughout this study, two common functionals (B3LYP[27,28] and M06-2X[29]) were used to assess the generality of the results. A wide range of basis sets was employed with these functionals to test whether results were artifacts of a particular computational methodology. The effect of polarization functions and diffuse functions on the calculations were also evaluated with multiple basis sets. Optimizations were typically carried out under aqueous conditions: solvation-free energy corrections were computed for aqueous solution using a self-consistent reaction field (SCRF) with either the IEFPCM[30,31] or SMD[32] solvation models. Unless indicated, all SCRF calculations were carried out using the UFF radii.[33] Vibrational analysis was used to confirm the identity of stationary points: the absence of imaginary frequencies indicates that the calculated structures exist at minima in the potential energy surface (PES). Transition-state optimizations were performed with the standard Berny[34] algorithm. In a few cases, we used the STQN[35] algorithm for transition state optimizations. The presence of a single imaginary frequency indicates an optimized transition state. This vibration must occur along the putative reaction coordinate. Where transition states could be located, intrinsic reaction coordinate (IRC) calculations were performed to confirm their identities.

Relaxed PES scans were performed starting from optimized structures. The same computational method was used to optimize the initial geometry and to generate these profiles. The carbon−carbon bond that is cleaved in the decarboxylation process was constrained at 0.1 Å iterations. Structures were optimized subject to this constraint. We assessed the effects of implementation of different levels of theory and basis sets on the calculated reaction profiles. Reaction profiles were generated with several different basis sets using the M06-2X or B3LYP level of theory. Ab initio calculations were also performed with the Møller−Plesset correlation correction (MP2).[36,37] We also benchmarked our reaction profile results against single point energy (SPE) calculations performed with CCSD[38,39] and the aug-cc-pVDZ basis set.[40]

The effects of explicit solvation were also considered. Relaxed PES scans were performed with ONIOM calculations. For these computations, the substrate was placed within an 18 Å × 18 Å × 18 Å water box. The bulk water was modeled with molecular mechanics (the UFF[33] or AMBER[41,42]), and the substrate was treated with the semiempirical PM3[43,44] or with B3LYP/6-31++G. The entire system was then optimized subject to a constrained carbon−carbon bond length.

The internal energy profiles were converted to free energy profiles by performing frequency calculations on each point of the relaxed PES scans. In general, the frequency calculations used to generate the thermochemical data are only valid at minima and saddle points.[45] However, frequency calculations of structures along the reaction coordinate (as is the case here) are often valid.[46] We also considered the possible effects of internal rotation modes[47] on the calculated free energy using the HinderedRotor keyword.

The thermodynamics of carboxylate hydration (Scheme 3) were computed by three related methods. In the "direct" method, the free

Scheme 3. Hydration of a Carboxylate Generates the Pre-Decarboxylation Intermediate

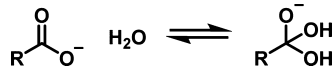

energy of hydration (ΔG°_{Hyd}) is simply the difference in free energy of the hydrated species and that of acetate and water. The work of Casado[48] shows that carbonyl hydration is modeled with far greater accuracy with a reference reaction (Scheme 4) where the equilibrium

Scheme 4. Isodesmic Reaction Used To Evaluate ΔG_{Hyd} for Substituted Acetates

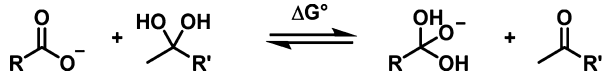

constant for hydration (K_{Hyd}) of the reference compound is known experimentally. The agreement between calculated K_{Hyd} with literature values is dependent on the structural similarity between the reference compound and the carbonyl of interest. As there are no available values for K_{Hyd} for carboxylates, we took two approaches to estimate those values: (1) The use of acetaldehyde as a reference (R′ = H in Scheme 4) gives fairly accurate results for all carbonyls studied[48] so we calculated ΔG°_{Hyd} using this approach. (2) Values of K_{Hyd} for acetic acid from the work of Guthrie[49] and the estimated pK_a of 1,1,1-ethanetriol[50,51] (see Supporting Information) make it possible to estimate ΔG°_{Hyd} for acetate using the thermodynamic cycle in Scheme 5. Hydration of acetate was then used as a reference reaction (R = O^- in Scheme 4).

For the analysis of hydration thermodynamics, structures were initially optimized in the gas phase at the M062X/6-31++G(d,p) or B3LYP/6-31++G(d,p) level. Single point energy (SPE) calculations were performed to obtain free energies of solvation (ΔG_{solv}) with both the PCM and the SMD solvation models. Though reoptimization in the solution phase does not significantly alter the calculated ΔG_{solv} for neutral species,[52] solution phase optimization of charged species is expected to give more accurate values for ΔG_{solv}.[53] We carried out

dx.doi.org/10.1021/jo501990u | J. Org. Chem. 2014, 79, 10972−10980

Scheme 5. Thermodynamic Cycle Used To Estimate ΔG_{Hyd} for Acetate

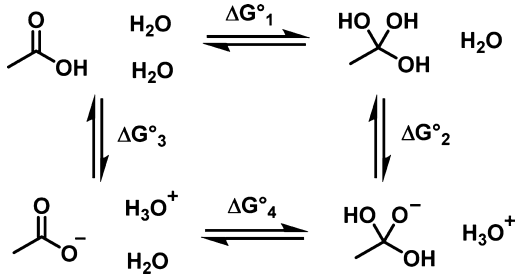

both SPE and solution phase optimizations in order to compare the results from those approaches. We also investigated the effects of different molecular cavities on ΔG_{solv} using the default UFF radii[33] and the UAHF radii[54] which have been shown to improve the performance of the PCM model.[32] In some cases, solution phase optimizations with the UAHF radii would not converge, even with repeated attempts. Occasional convergence problems with the united atom radii models are known.[54−56] As an alternative, solution-phase SPE calculations of structures optimized in the gas phase were used. We evaluated the performance of the density functional and atomic radii models used in the SCRF calculation by comparing the calculated free energy of hydration of acetaldehyde to the experimentally determined value.

RESULTS AND DISCUSSION

We initially attempted to model the decarboxylation of trichloroacetate along the intrinsic reaction coordinate (IRC). However, our attempts to locate a transition state with established algorithms (Berny,[34] STQN[35]) were unsuccessful. We then used relaxed PES scans as an alternative to characterize the reaction.[14] The resulting profiles (Figure 1)

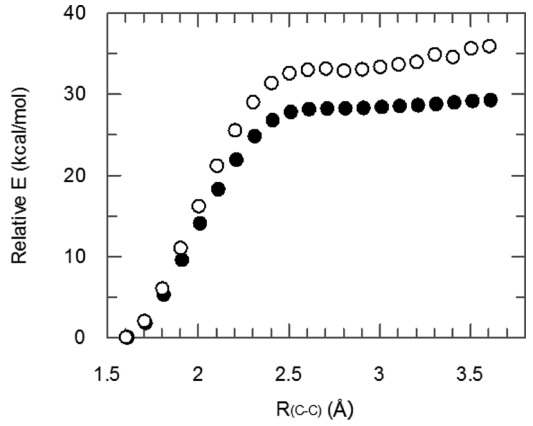

Figure 1. Reaction profiles for the decarboxylation of TCA by dissociation of trichloromethyl anion and CO_2. Calculations performed at the M06-2X/6-31++G(d,p)/SMD (○) and the B3LYP/6-31++G(d,p)/SMD (●) level.

clearly show why no transition state could be located: there is no saddle-point on the PES corresponding to a transition state that is an acceptable activated complex. Instead, the energy of the system rises to a plateau and continues to rise with increasing distances between the trichloromethide and CO_2.

The lack of an energetic minimum corresponding to the formation of the products suggests that substantial separation of the resulting carbanion and CO_2 would be necessary to facilitate their actual formation as separately solvated products. At each point along this plateau, separation is in competition with the barrier-free recombination of the species to give trichloroacetate. Even where the species are 4.0 Å apart, there is no barrier to their recombination, suggesting that solvent molecules would be unable to intervene to allow separation. This is reminiscent of the situations where carbocation formation is hindered by significant internal return of the leaving group in a solvolytic reaction.[57−61] This situation produces a compelling need for a mechanistic alternative to explain the existence of the overall observed decarboxylation of TCA.

These profiles also show a clear dependence of the energy plateau on the functional employed. The reaction profile calculated with the B3LYP functional exhibits a significantly lower energy plateau than the profile generated with the M06-2X functional. This is consistent with literature reports suggesting the B3LYP functionals substantially underestimate barrier heights for many reactions.[29,62−64] These reports also suggest that the M06-2X functional more accurately predicts reaction barriers and main-group thermochemistry.[29,62−64]

As indicated in the Computational Methods section, we used many combinations of density functionals and basis sets to generate similar reaction profiles (available in the Supporting Information). In no case did we observe a substantial barrier to the recombination. The reaction profiles were also not significantly impacted by the addition of diffuse and/or polarization functions. In all the profiles there is a negligible barrier to recombination (<0.5−1 kcal/mol) resulting from application of any basis set, which suggests that these calculations accurately represent the PES of the reaction.

Explicit Solvation Using ONIOM Calculations. We attempted to address potential shortcomings in the computational methodology that could have produced the PES scans in the form we observe. One alternative explanation for the lack of an energetic minimum corresponding to products is the inadequacy of implicit solvation to mimic specific interactions between the solvent and solutes. Implicit solvation models operate on the assumption that solute−solvent interactions are independent of the structure of the solvent and can be modeled from the dielectric constant of the bulk medium alone.[65−67] We performed numerous calculations to assess the effect of explicit solvation on the generated reaction profile for the decarboxylation of TCA.

The reaction profile generated with an ONIOM calculation at the PM3//UFF level has an energy plateau of about 20 kcal/mol and shows negligible energetic relaxation upon further stretching of the carbon−carbon bond that is to be cleaved (Supporting Information, Figure S3a). While this calculation includes explicit solvation, the treatment of solute−solvent hydrogen bonds by both levels of theory may be too simplistic. Outside of hydrogen bonds closely related to those found in its training set, the PM3 method has been found to underestimate hydrogen bond and other noncovalent interaction energies.[68] Further, the UFF force field models hydrogen bonds with an explicit Lennard-Jones 6-12 type term.[33] This methodology can predict electrostatic interactions with moderate accuracy but was not parametrized for the type of H-bond likely to arise in the loss of CO_2 from the trichloromethyl anion (ie. water as an H-bond donor to an explicit carbanion).

Another ONIOM calculation was performed at the B3LYP/6-31++G//AMBER level. DFT methods are known to predict hydrogen bond strength with more accuracy than the MNDO methods.[69] The AMBER force field uses a combination of a Lennard-Jones 6−12 term and a Coulombic interaction term to

dx.doi.org/10.1021/jo501990u | J. Org. Chem. 2014, 79, 10972−10980

model noncovalent interactions.[42] This approach has been shown to treat hydrogen bonding with reasonable accuracy.[70] Despite the ability of these levels of theory to model hydrogen bonding, the generated PES scan (Supporting Information, Figure S3b) exhibits no barrier to recombination of the trichloromethyl anion with CO_2. Examination of the optimized structures along the scan gives no indication of any H-bonding interaction between water molecules and the trichloromethyl anion.

The protonation of trichloromethyl anion by water is known to be extremely fast[23] and this process would clearly prevent its recombination with CO_2. From our initial studies of the reaction with explicit solvation, it appeared that the bent hydrogen bond between the solvent and the trichloromethyl anion cannot form while the carbanion is associated with CO_2. It is possible that the electrostatic interaction of the proximal CO_2 with the trichloromethyl anion (at least in part) quenches the H-bond-accepting ability of the carbanion. If CO_2 were able to diffuse to more substantial distances, the protonation of the carbanion would necessarily occur at a rate equal to that which has been reported for the protonation of free trichloromethyl anion.

We assessed this possibility by extending the reaction profile to further C−C distances. The effect of DFT-modeled water was evaluated as well. The resulting profiles are not significantly different over a 4 Å C−C bond distance. However, the optimized structures with a constrained bond length around 4.2 Å clearly show a bent hydrogen bond between the carbanion and a DFT-modeled water. This interaction results in a 5 kcal/mol drop in energy along the reaction profiles (Supporting Information, Figure S3c,d). With continued increase in the distance between the CO_2 and trichloromethyl anion, a gradual increase in energy is observed. This appears to be caused by disruption of the solvent network as no water molecules separate the reactive pair at any point along the profile. As the trichloromethyl anion and CO_2 exist within the same solvent shell and no specific solvent−solute interactions develop while these species are associated ($R_{C-C} \leq 4$ Å), diffusion to such a distance will not occur as recombination is a barrier-free process.

Free Energy Reaction Profiles. The relaxed PES scans presented thus far measure internal energy of the trichloroacetate as a function of the carbon−carbon bond. We have also considered the Gibbs free energy change as a function of this bond length. Cleary, the decarboxylation of TCA is entropically favorable. It may be that the entropic contribution to the free energy change introduces a significant barrier to the recombination of CO_2 and the trichloromethyl anion. This is especially important because there are reactions known to have no enthalpic relaxation following the canonical transition state.[71−73] The reactions that have significant entropic (and thus free energy) barriers are classified as being entropically controlled. Variational transition state theory was developed by Truhlar to describe such a situation quantitatively.[74]

We calculated the thermodynamic properties of trichloroacetate at each point along the previously presented reaction profiles for loss of CO_2 from TCA. The resulting Gibbs free energy profiles (Figure 2) at 298 K do not differ significantly from the internal energy reaction profiles. The apparent "noise" in the free energy profiles is likely a consequence of performing frequency calculations on nonstationary points. The free energy obtained from frequency calculations using the Hindered Rotor keyword are essentially identical. These results indicate that the frequency calculations are providing thermochemical data that are sufficiently accurate.

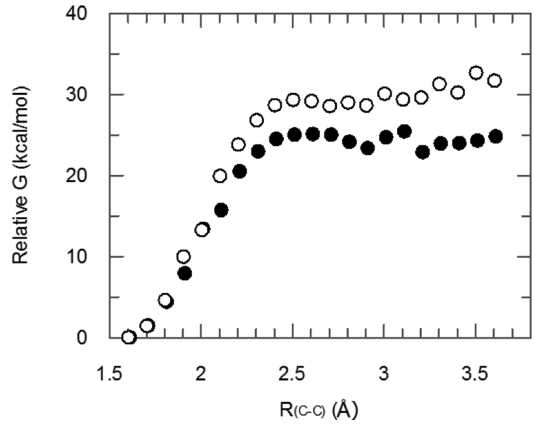

Figure 2. Free energy profiles for the decarboxylation of TCA by dissociation of trichloromethyl anion and CO_2. Calculations performed at the M06-2X/6-31++G(d,p)/SMD (○) and the B3LYP/6-31++G(d,p)/SMD (●) level.

The agreement between the computed reaction barriers and those for the experimentally observed rate constants[19] vary with the density functional, basis set and solvation model. Table 1 summarizes the energetics for the direct loss of CO_2 from trichloroacetate. As transition states could not be located, the parameters represent the differences between the ground state and the energetic plateau. The B3LYP functional routinely underestimates the magnitude of the reaction barrier. This result is in agreement with previous reports on the performance of the functional.[29,64,75,76] The M06-2X functional has been shown to predict barrier heights much more accurately[29,64] and gives better agreement with experimental results. We also find that the SMD solvation model gives better agreement than the PCM model. This is likely because the training set of the SMD model includes a large number of charged species[32] and is more appropriately parametrized to handle ionic species.

Table 1. Calculated Parameters for the Loss of CO_2 from Trichloroacetate[a]

	B3LYP		M062X		
	PCM	SMD	PCM	SMD	exptl[19]
$\Delta H^{\ddagger b}$	19.3	26.2	24.2	31.6	32.6
$\Delta G^{\ddagger b}$	18.0	25.0	21.0	29.3	28.1

[a]All calculations were carried out with the 6-31++G(d,p) basis set. [b]No TS could be located. These values (in kcal/mol) represent the change from ground state to the energetic plateau.

Benchmarked Reaction Profiles. The CCSD-calculated energies from the reaction profile structures are shown in Figure 3. This level of theory is computationally costly but yields very accurate barrier heights.[62,64,75] The apparent energy of activation obtained with this methodology (approximately 25.0 kcal/mol) is in reasonable agreement with the experimental results and gives further support for the accuracy of our free energy profiles. These show slightly more pronounced barriers to recombination. However, these barriers are less than 2 kcal/mol, which suggests that the recombination will compete effectively with solvation and separation. The reverse reaction is especially problematic as the system does not relax as the bond becomes longer. Therefore, the moderate

dx.doi.org/10.1021/jo501990u | J. Org. Chem. 2014, 79, 10972−10980

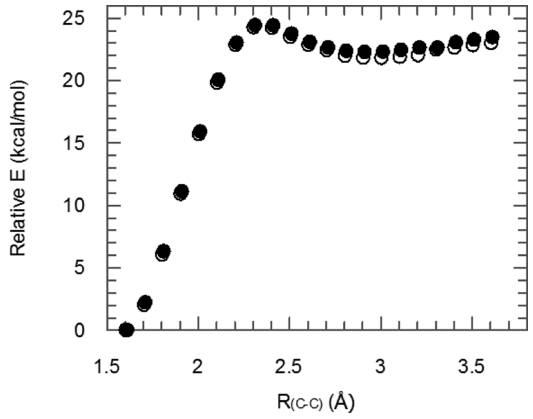

Figure 3. Reaction profile for the loss of CO_2 from trichloroacetate generated with CCSD/aug-cc-pvdz/SMD. Single point energy calculations were performed on TCA structures optimized with M06-2X/6-31++G(d,p)/SMD (○) and the B3LYP/6-31++G(d,p)/SMD (●) level.

increase in separation distance does not provide any stabilization of the potential products.

Effect of Carbanion Basicity on Recombination Barrier. We also considered to what extent variation in the basicity of the incipient carbanion could introduce a barrier to its combination with CO_2. Thus, reaction profiles were generated for other halogenated acetates (Figure 4). Not

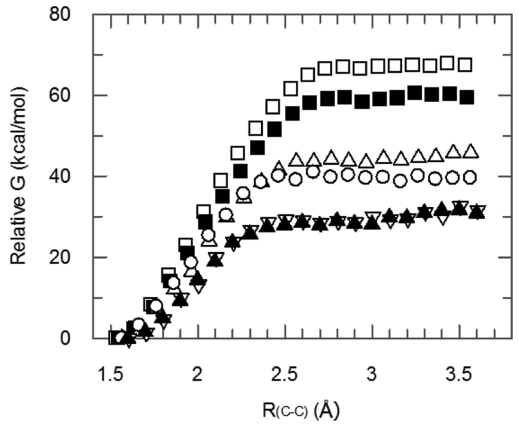

Figure 4. Reaction profiles for the loss of CO_2 from acetate (□), MCA (■), DCA (△), TCA (▽), TFA (○) and TBA (▲). All calculations were performed with M06-2X/6-31++G(d,p)/SMD. The recombination of the carbanion with CO_2 is barrierless in all cases.

surprisingly, the magnitude of the free energy change increases in proportion to the energy of the incipient carbanion. The carbanions are stabilized to different degrees but all remain nucleophilic and can react with CO_2. This is reflected by the varying energetic maxima and the absence of barriers to recombination. From the profiles in Figure 4, it is clear that the decarboxylation reactions of these compounds also cannot proceed by the one-step process. The highly energetic nature of the carbanions also present increased barriers compared to the reaction of TCA.

Hydration: A Necessary Mechanistic Alternative. While we attempted to address the possible computational oversights that could result in the negligible observed barrier to recombination, we noted that our results are consistent with the results of Gao and Major, where the lack of such a barrier in the decarboxylation of *N*-methyl picolinate is described as "a characteristic feature of this class of decarboxylation reaction".[10,15] However, those authors did not consider an alternative pathway.

Taken together with previous reports,[77−79] these results lead us to conclude that decarboxylation pathways that produce localized carbanions by direct formation of CO_2 are unavoidably reversible. As the trichloromethyl anion is necessarily localized, the computed reaction profiles accurately describe the potential energy surface for its simultaneous formation along with CO_2 from TCA. On the basis of this evidence, the decarboxylation of TCA cannot proceed without the existence of an alternative route involving at least one intermediate. An alternative associative mechanism overcomes the intrinsic internal return by changing the leaving group to the less electrophilic bicarbonate ion or carbonic acid as we have observed for the related decarboxylation process of mandelylthiamin.[3]

Thermodynamics of Carboxylate Hydration. A key component of the associative route to decarboxylation is the formation of the carboxyl hydrate. While there have been many studies on the covalent hydration of aldehydes, ketones,[80−85] esters, and carboxylic acids,[49,51,86−88] there are few reports of carboxylate hydration. One important example was reported by Llewellyn and O'Connor. They determined the rate constants for ^{18}O exchange from labeled water into a variety of carboxylate groups that occur via formation of hydrates.[89−92] While those kinetic studies give strong evidence that carboxylate hydration is a viable step along a reaction pathway, there has been no study of the thermodynamics of the process.

Frequency calculations performed on the optimized structures indicate that all of the hydrated acetates exist at stationary points. No extraneous measures were necessary to reach convergence. The free energies of hydration as calculated with the direct method using the acetaldehyde reference and the acetate reference are summarized in Table 2. Regardless of the method, we find that increased electronegativity of the R group facilitates hydration. This trend is in agreement with the observed rate of ^{18}O incorporation into halogenated acetates from addition of $H_2{}^{18}O$.[89,90]

The inadequacy of the direct calculation is made immediately apparent by comparing the experimental value for acetaldehyde hydration (ΔG_{Hyd} = −0.041 kcal/mol[80−83]) with the calculated values. Where this method is used, the resulting ΔG_{Hyd} values are strongly dependent on the solvation model. Both the PCM and SMD models overestimate ΔG_{Hyd}, although the latter model comes much closer to the experimental energy. This is a reasonable expectation since the SMD model was shown to give more accurate solvation free energies for both neutral and ionic species in water.[32] The excellent performance of the SMD model in predicting solvation free energies of the chemically diverse SAMPL1 set[93,94] also indicates the predictive ability of this solvent model.

The substantial disagreement between the free energies of hydration calculated directly with the B3LYP or M06-2X functionals further illustrates the shortcomings of this method. The B3LYP functional consistently overestimates the hydration free energy of acetaldehyde and predicts ΔG_{Hyd} values 6−10 kcal/mol higher than the M06-2X functional does. This discrepancy is likely due to each functional's introduction of systematic errors arising from differential solvation and solute−solvent hydrogen bonding on either side of the hydration equilibrium.[48] These errors are exacerbated when structures are

dx.doi.org/10.1021/jo501990u | J. Org. Chem. 2014, 79, 10972−10980

Table 2. Free Energies of Hydration (ΔG_{Hyd}) of Acetates Calculated with Various Computational Methodologies

	B3LYP/6-31++G(d,p)								M062X/6-31++G(d,p)							
	SPE				reoptimized				SPE				reoptimized			
	PCM		SMD		PCM		SMD		PCM		SMD		PCM		SMD	
compd	UFF	UAHF	UFF	UAHF	UFF	UAHF	UFF	UAHF	UFF	UAHF	UFF	UAHF	UFF	UAHF	UFF	UAHF
Direct[a] Calculation Method																
acetate	33.4	33.4	33.5	30.8	33.5	32.1	34.0	29.2	27.1	26.6	26.3	24.3	27.2	24.1	26.8	9.7
MCA	34.6	33.9	33.5	31.7	34.3	31.7	33.1	29.2	24.8	24.0	24.8	21.5	26.0	23.4	25.1	9.2
DCA	31.2	32.0	30.8	29.7	33.5	28.4[d]	31.3	26.2[d]	22.5	22.4	21.7	20.2	23.6	19.2[d]	22.7	5.2[d]
TCA	29.8	26.5	30.9	24.3	32.1	27.0	30.9	24.5	21.9	17.2	21.6	14.9	22.9	16.7	21.3	3.1
TFA	29.9	27.6	30.0	25.6	30.9	26.0	29.1	23.4	21.5	17.3	22.2	15.0	22.8	17.6	21.1	2.4
TBA	27.6	24.0	28.3	21.8	29.4	24.4	29.7	21.9	17.8	12.8	18.0	10.8	19.9	15.6	20.9	1.8
acetaldehyde	11.0	3.1	11.6	1.2	10.6	4.5	11.6	3.1	4.6	−3.9	3.9	−5.3	4.9	−2.4	4.1	−5.4
Acetaldehyde Reference[b] Calculation Method																
acetate	22.3	30.2	21.8	29.5	22.9	27.5[e]	22.3	26.1[e]	22.5	30.4	22.3	29.5	22.2	26.4[e]	22.6	31.6
MCA	23.6	30.7	21.9	30.4	23.7	27.1[e]	21.4	26.1[e]	20.2	27.8	20.8	26.7	21.0	25.7[e]	20.9	31.1
DCA	20.2	28.8	19.1	28.5	22.9	30.6[e]	19.7	23.1[e]	17.9	26.3	17.7	25.4	18.6	21.6[e]	18.6	27.1
TCA	18.8	23.3	19.3	23.0	21.5	22.5[e]	19.3	21.4[e]	17.2	21.0	17.7	20.1	18.0	19.0[e]	17.2	25.0
TFA	18.8	24.4	18.3	24.4	20.2	21.4[e]	17.5	20.3[e]	16.9	21.2	18.3	20.2	17.9	19.9[e]	16.9	24.3
TBA	16.6	20.8	16.6	20.5	18.7	19.9[e]	18.0	18.8[e]	13.1	16.7	14.1	16.0	15.0	17.9[e]	16.7	23.7
Acetate Reference[c] Calculation Method																
MCA	23.8	23.0	22.6	23.4	23.3	22.1	21.6	22.6	20.2	19.9	20.9	19.7	21.3	21.8	20.8	22.0
DCA	20.3	21.1	19.8	21.5	22.5	18.9	19.9	19.5	17.9	18.3	17.9	18.4	18.9	17.6	18.5	18.0
TCA	18.9	15.6	20.0	16.0	21.1	17.5	19.5	17.9	17.2	13.1	17.8	13.1	18.2	15.2	17.0	15.9
TFA	19.0	16.7	19.0	17.4	19.8	16.4	17.7	16.8	16.9	13.2	18.4	13.2	18.1	16.0	16.8	15.2
TBA	16.8	13.1	17.3	13.5	18.3	14.9	18.2	15.2	13.2	8.7	14.2	9.0	15.3	14.0	16.6	14.6

[a]Calculated ΔG_{Hyd} from free energy values of the optimized acetate (G°_{RCOO}), hydrate (G°_{RHyd}), and water (G°_{H2O}) with $\Delta G_{Hyd} = G^\circ_{RHyd} - G^\circ_{RCOO} - G^\circ_{H2O}$. [b]Used acetaldehyde hydration (ΔG° = −0.041 kcal/mol[80−83]) as the reference reaction as described in the text. [c]Used acetate hydration and the estimated free energy change (ΔG° = 22.5 kcal/mol) as the reference reaction as described in the text. [d]Optimization of DCA did not converge. SPE values were used in place of reoptimized free energies. [e]Solution phase optimization of hydrated acetaldehyde with the UAHF radii did not converge. SPE values were used in place of reoptimized free energies. All values are given in kcal/mol.

reoptimized with the SMD/UAHF solvent model. This computational methodology produces an average difference of 20 kcal/mol! While the calculated ΔG_{Hyd} for acetaldehyde suggests the M06-2X functional is better suited for carbonyl hydration, the widespread nature of the values confirms that the direct calculation of hydration free energy will not give meaningful results.

The energetics calculated with the acetaldehyde reference illustrate how use of a reference reaction drastically reduces the systematic errors discussed earlier. Values of ΔG_{Hyd} calculated with this method show a much less significant dependency on the functional employed. In fact, there is no statistically significant difference between ΔG_{Hyd} values calculated with either functional using the acetaldehyde reference. However, the choice of atomic radii still has a large influence on the free energies of hydration. This dependence is likely due to the different charge states of the carboxylate and the reference reaction, since solvation free energies of ionic species are more accurately computed with the UAHF radii.[53]

Using the hydration of acetate as a reference reaction, we arrive at ΔG_{Hyd} values that are relatively invariant with regard to choice of functional, solvent model, and atomic radii. This indicates that use of a structurally similar reference compound minimizes the amount of systematic error introduced into these calculations. On the basis of these results and Casado's study,[48] the free energies of hydration obtained with the acetate reference reaction are likely to be the most accurate. The largest discrepancy within this calculation method seems to be the choice of radii employed in the SCRF calculation. Table 3 summarizes the averaged results and the spread of the

Table 3. Averaged Free Energies of Hydration According to Radii Used in the SCRF Calculation[a]

	B3LYP/6-31++G**		M062X/6-31++G**	
compd	UFF	UAHF	UFF	UAHF
MCA	22.8 ± 1.0	22.8 ± 0.6	20.8 ± 0.5	20.9 ± 1.2
DCA	20.6 ± 1.3	20.2 ± 1.2	18.3 ± 0.5	18.1 ± 0.4
TCA	19.9 ± 0.9	16.8 ± 1.1	17.6 ± 0.6	14.3 ± 1.4
TFA	18.9 ± 0.9	16.8 ± 0.4	17.6 ± 0.8	14.4 ± 1.4
TBA	17.7 ± 0.7	14.2 ± 1.0	14.8 ± 1.5	11.6 ± 3.2

[a]All values in kcal/mol.

calculated free energies of hydration. Since the UAHF model is more accurate in predicting acidities[56,95] and free energies of solvation,[96,97] it is reasonable to assume that the values calculated with the UAHF model more closely resemble the true free energies of hydration.

A potential source of error in the calculation of the hydration energetics is the inability of either solvent model to represent the hydration of the triol-like species accurately. The solvent models employed are parametrized against experimentally available ΔG_{solv}, and neither model includes hydrated carbonyls in the training sets.[30,32,98] To evaluate the ability of these solvent models to treat solvation of the hydrated species accurately, we calculated the pK_a of the triol using an isodesmic proton transfer between this species and a base of known pK_a.[99−101] The calculated pK_a is in good agreement with the value estimated from linear free energy relationships (see

dx.doi.org/10.1021/jo501990u | J. Org. Chem. 2014, 79, 10972−10980

Supporting Information), indicating that the implicit models are appropriately treating solvation of the hydrated species.

Decarboxylation Profiles from the Hydrate. While the hydration of carboxylates is clearly an endergonic reaction, the previous reports of ^{18}O-exchange[89−92] and the computational results presented here indicate that the hydrated species is a competent mechanistic intermediate. These species can then be utilized as the starting points for evaluation of the hydrolytic decarboxylation of halogenated acetates. The reaction profiles are generated identically to those previously reported. Comparing the reaction profiles for the decarboxylation from TCA (Figure 1) and the TCA hydrate (Figure 5) illustrates the

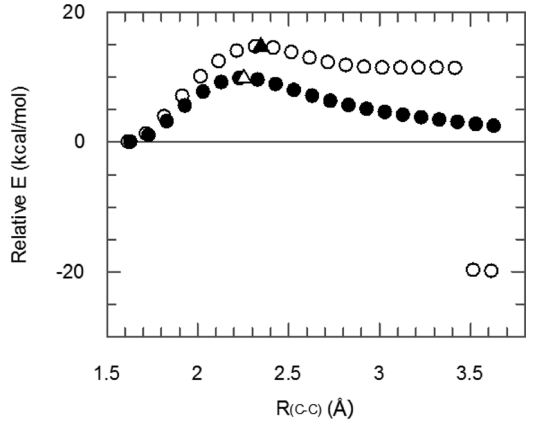

Figure 5. Reaction profiles for the decarboxylation of TCA hydrate. Calculations performed at the M06-2X/6-31++G(d,p)/PCM (○) and the B3LYP/6-31++G(d,p)/PCM (●) level. Transition states located with M06-2X/6-31++G(d,p)/PCM (△) and B3LYP/6-31++G(d,p)/PCM (▲).

advantage of adding water to the reactant prior to C−C cleavage. This pathway produces the trichloromethyl anion and carbonic acid rather than CO_2. The former is a much less reactive electrophile than the latter. This is seen in the substantial barrier observed in the reaction profile in Figure 5 compared to that in Figure 1. The corresponding free energy profile (Figure 6) also shows a substantial relaxation when a critical distance between the trichloromethyl anion and the leaving group is reached.

Transition state structures were easily located for the hydrated acetates. Vibrational analysis confirmed that the structures were located at saddle points and the lone imaginary frequency corresponded to carbon−carbon bond cleavage. In addition, the optimized transition states are in good agreement with the generated reaction profiles. IRC calculations performed from these transition states trace the generated reaction profiles, illustrating the appropriateness of using relaxed PES scans as reaction profile models. In solution, removal of a proton from the intermediate facilitates the reaction by producing bicarbonate in concert with C−C cleavage, leading to the observation of catalysis by base. In that case, undissociated carbonic acid would be too acidic to form directly in a basic solution.

Total $\Delta G^{\ddagger}$ and the benefit of the hydrolytic pathway. As transition states along the hydrolytic path are easily located, a true $\Delta G^{\ddagger}$ can be calculated and compared to the results of Verhoek.[19] The calculated free energies of activation for the hydrolytic decarboxylation of TCA are summarized in Table 4. These values represent the Gibbs free energy change on going

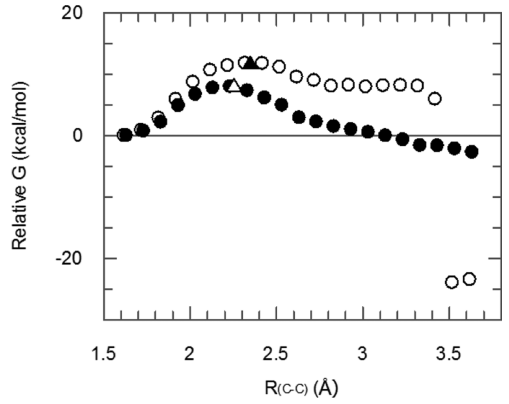

Figure 6. Free energy profiles for the decarboxylation of TCA hydrate. Calculations performed at the M06-2X/6-31++G(d,p)/PCM (○) and the B3LYP/6-31++G(d,p)/PCM (●) level. Transition states located with M06-2X/6-31++G(d,p)/PCM (△) and B3LYP/6-31++G(d,p)/PCM (▲).

Table 4. Free Energy of Activation for the Hydrolytic Decarboxylation of TCA[a]

	B3LYP		M062X		
	PCM	SMD	PCM	SMD	exptl[18]
$\Delta G^{\ddagger}$	24.7	28.0	25.9	31.6	28.1

[a]All calculations were carried out with the 6-31++G(d,p) basis set.

from TCA to the hydrated transition state and use the free energy of hydration from the UAHF calculations. A comparison of $\Delta G^{\ddagger}$ from Tables 1 and 4 shows that the free energies of activation for both reaction pathways are in good agreement with the observed rate constants. Both pathways appear to have roughly equal free energies of activation. However, the hydrolytic pathway has the added benefit of introducing a barrier to the recombination of the trichloromethyl anion and the departing electrophile.

It is clear that the hydration pathway that avoids the formation of CO_2 along with a carbanion is not restricted to the decarboxylation of TCA. In general, direct formation of carbon dioxide can be unproductive because solvation of CO_2 fails to compete with recombination with the carbanion. Hydration prior to bond cleavage provides an alternative pathway where trapping of CO_2 has occurred ahead of its formation. The resulting carbonic acid species is readily solvated but can readily undergo conversion to CO_2 and water.[102] Kinetically, this would be consistent with direct decarboxylation as the stoichiometry of solvent water in the reaction does not appear in the observed rate law. It is only through the presence of base catalysis that the hydrolytic pathway becomes apparent.

In cases where the resulting carbanion is ultimately delocalized, hydration pathways can still facilitate the reaction by the preferred solvation of the hydrated product. We also know from application of the principle of nonperfect synchronization[103,104] that formation of CO_2 can occur ahead of delocalization of the accompanying carbanion. To the extent that the carbanion remains localized, internal return is also likely to be significant,[105] leading to the potential general importance of the hydration pathway.

Our results are consistent with observations on the nature of enzymic reactions that cleave carboxyl groups. Decarboxylases have been reported that appear to have evolved to produce carbonic acid derivatives[106] in parallel with amide hydrolases[5]

dx.doi.org/10.1021/jo501990u | J. Org. Chem. 2014, 79, 10972−10980

and serine proteases.[107] These pathways overcome the problem of internal return by converting the putative CO_2 to a less reactive leaving group. An alternative strategy to avoid internal return would involve concerted protonation of the incipient carbanion.[108,109] Recent work by Major[110] suggests that orotidine 5′-monophosphate decarboxylase uses this strategy to facilitate direct decarboxylation. Both pathways indicate the problem of internal return in decarboxylation reactions and can be applied to a variety of what have been considered to be energetically challenging enzyme-catalyzed decarboxylation reactions.[111−114]

CONCLUSIONS

On the basis of our analysis of the decarboxylation of trichloroacetate we see how hydration of a carboxyl group prior to decarboxylation overcomes an intrinsic problem in decarboxylation reactions that produce CO_2 directly. This result is consistent with base catalysis of the decarboxylation of trichloroacetate[22] and of mandelylthiamin[3] as well as reported nucleophilic addition mechanisms in enzymic decarboxylation reactions.[105−107] In addition, reactions involving bicarbonate in catalyzed carboxylation processes[105,115] are implicated by application of the principle of microscopic reversibility.

ASSOCIATED CONTENT

Supporting Information

Full citation for ref 26. Reaction profiles generated with various levels of theory and basis sets. B3LYP and M06-2X coordinates and thermodynamics of optimized structures. IRC results. Estimation of the pK_a of 1,1,1-ethanetriol and the free energy of acetate hydration. Potential energy surfaces for the loss of carbon dioxide and carbonic acid from TCA. This material is available free of charge via the Internet at http://pubs.acs.org.

AUTHOR INFORMATION

Corresponding Author

*E-mail: r.kluger@utoronto.ca.

Notes

The authors declare no competing financial interest.

ACKNOWLEDGMENTS

This work was supported by NSERC Canada through a Discovery Grant. G.W.H. is the grateful recipient of a postgraduate scholarship from NSERC. This work was made possible by the facilities of the Shared Hierarchical Academic Research Computing Network (SHARCNET) and Compute/Calcul Canada.

REFERENCES

(1) Brown, B. R. *Q. Rev. Chem. Soc.* **1951**, *5*, 131.
(2) Clark, L. W. In *The Chemistry of Carboxylic Acids and Esters*; Patai, S., Ed.; John Wiley & Sons, Ltd.: London, 1969.
(3) Howe, G. W.; Bielecki, M.; Kluger, R. *J. Am. Chem. Soc.* **2012**, *134*, 20621.
(4) Brandt, G. S.; Kneen, M. M.; Chakraborty, S.; Baykal, A. T.; Nemeria, N.; Yep, A.; Ruby, D. I.; Petsko, G. A.; Kenyon, G. L.; McLeish, M. J.; Jordan, F.; Ringe, D. *Biochemistry* **2009**, *48*, 3247.
(5) Xu, S.; Li, W.; Zhu, J.; Wang, R.; Li, Z.; Xu, G. L.; Ding, J. *Cell Res.* **2013**, *23*, 1296.
(6) Carroll, J. J.; Slupsky, J. D.; Mather, A. E. *J. Phys. Chem. Ref. Data* **1991**, *20*, 1201.
(7) Duan, Z.; Sun, R. *Chem. Geol.* **2003**, *193*, 257.
(8) Sato, H.; Matubayasi, N.; Nakahara, M.; Hirata, F. *Chem. Phys. Lett.* **2000**, *323*, 257.
(9) Hu, H.; Boone, A.; Yang, W. *J. Am. Chem. Soc.* **2008**, *130*, 14493.
(10) Gao, J.; Ma, S.; Major, D. T.; Nam, K.; Pu, J.; Truhlar, D. G. *Chem. Rev.* **2006**, *106*, 3188.
(11) Wu, N.; Mo, Y. R.; Gao, J. L.; Pai, E. F. *Proc. Natl. Acad. Sci. U.S.A.* **2000**, *97*, 2017.
(12) Raugei, S.; Cascella, M.; Carloni, P. *J. Am. Chem. Soc.* **2004**, *126*, 15730.
(13) Stanton, C. L.; Kuo, I. W.; Mundy, C. J.; Laino, T.; Houk, K. N. *J. Phys. Chem. B* **2007**, *111*, 12573.
(14) Singleton, D. A.; Merrigan, S. R.; Kim, B. J.; Beak, P.; Phillips, L. M.; Lee, J. K. *J. Am. Chem. Soc.* **2000**, *122*, 3296.
(15) Major, D. T.; Gao, J. *J. Chem. Theory Comput.* **2007**, *3*, 949.
(16) Lee, G. K.; Houk, K. N. *Science* **1997**, *276*, 942.
(17) Kemp, D. S.; Paul, K. G. *J. Am. Chem. Soc.* **1975**, *97*, 7305.
(18) Gao, J. *J. Am. Chem. Soc.* **1995**, *117*, 8600.
(19) Verhoek, F. H. *J. Am. Chem. Soc.* **1934**, *56*, 571.
(20) Bigeleisen, J.; Allen, T. L. *J. Chem. Phys.* **1951**, *19*, 760.
(21) Dumas, J. B. A. *C. R. Acad. Sci.* **1839**, *9*, 813. Leicester, H. M.; Klickstein, H. S. *A Source Book in Chemistry 1400−1900 (Engl. Transl.)*; Harvard University Press: Cambridge, 1952. "By treating [TCA] with any alkali I have obtained a very remarkable reaction. The acid is converted into two new substances, namely carbonic acid, which is combined with the alkali, and chloroform, which is liberated."
(22) Urbansky, E. T. *Chem. Rev.* **2001**, *101*, 3233.
(23) Lin, A. C.; Chiang, Y.; Dahlberg, D. B.; Kresge, A. J. *J. Am. Chem. Soc.* **1983**, *105*, 5380.
(24) Battino, R.; Clever, H. L. *Chem. Rev.* **1966**, *66*, 395.
(25) Houghton, G.; McLean, A. M.; Ritchie, P. D. *Chem. Eng. Sci.* **1957**, *6*, 132.
(26) *Gaussian 09, Revision D.01*; Frisch, M. J.; et al. Gaussian, Inc.: Wallingford, CT, 2009.
(27) Becke, A. D. *J. Chem. Phys.* **1993**, *98*, 5648.
(28) Kim, K.; Jordan, K. D. *J. Phys. Chem.* **1994**, *98*, 10089.
(29) Zhao, Y.; Truhlar, D. G. *Theor. Chem. Acc.* **2008**, *120*, 215.
(30) Miertuš, S.; Scrocco, E.; Tomasi, J. *Chem. Phys.* **1981**, *55*, 117.
(31) Scalmani, G.; Frisch, M. J. *J. Chem. Phys.* **2010**, *132*, 114110.
(32) Marenich, A. V.; Cramer, C. J.; Truhlar, D. G. *J. Phys. Chem. B* **2009**, *113*, 6378.
(33) Rappé, A. K.; Casewit, C. J.; Colwell, K. S.; Goddard, W. A.; Skiff, W. M. *J. Am. Chem. Soc.* **1992**, *114*, 10024.
(34) Schlegel, H. B. *J. Comput. Chem.* **1982**, *3*, 214.
(35) Peng, C.; Ayala, P. Y.; Schlegel, H. B. *J. Comput. Chem.* **1996**, *17*, 49.
(36) Pople, J. A.; Krishnan, R.; Schlegel, H. B.; Binkley, J. S. *Int. J. Quantum Chem.* **1979**, *13*, 225.
(37) Frisch, M. J.; Head-Gordon, M.; Pople, J. A. *Chem. Phys. Lett.* **1990**, *166*, 281.
(38) Purvis, G. D.; Bartlett, R. J. *J. Chem. Phys.* **1982**, *76*, 1910.
(39) Scuseria, G. E.; Schaefer, H. F. *J. Chem. Phys.* **1989**, *90*, 3700.
(40) Dunning, T. H., Jr. *J. Chem. Phys.* **1989**, *90*, 1007.
(41) Weiner, P. K.; Kollman, P. A. *J. Comput. Chem.* **1981**, *2*, 287.
(42) Cornell, W. D.; Cieplak, P.; Bayly, C. I.; Gould, I. R.; Merz, J. K. M.; Ferguson, D. M.; Spellmeyer, D. C.; Fox, T.; Caldwell, J. W.; Kollman, P. A. *J. Am. Chem. Soc.* **1995**, *117*, 5179.
(43) Stewart, J. J. P. *J. Comput. Chem.* **1989**, *10*, 209.
(44) Stewart, J. J. P. *J. Comput. Chem.* **1989**, *10*, 221.
(45) Ochterski, J. W. Gaussian. Gaussian, Inc.: Wallingford, CT, 2000.
(46) Ochterski, J. W. Gaussian. Gaussian, Inc.: Wallingford, CT, 2000.
(47) Ayala, P. Y.; Schlegel, H. B. *J. Chem. Phys.* **1998**, *108*, 2314.
(48) Gómez-Bombarelli, R.; González-Pérez, M.; Pérez-Prior, M. T.; Calle, E.; Casado, J. *J. Phys. Chem. A* **2009**, *113*, 11423.
(49) Guthrie, J. P. *J. Am. Chem. Soc.* **1973**, *95*, 6999.
(50) Guthrie, J. P. *J. Am. Chem. Soc.* **1978**, *100*, 5892.
(51) Guthrie, J. P. *J. Am. Chem. Soc.* **2000**, *122*, 5529.

(52) Namazian, M.; Halvani, S.; Noorbala, M. R. *THEOCHEM* **2004**, *711*, 13.
(53) Schüürmann, G.; Cossi, M.; Barone, V.; Tomasi, J. *J. Phys. Chem. A* **1998**, *102*, 6706.
(54) Barone, V.; Cossi, M.; Tomasi, J. *J. Chem. Phys.* **1997**, *107*, 3210.
(55) Kraka, E.; Cremer, D.; Koller, J.; Plezničar, B. *J. Am. Chem. Soc.* **2002**, *124*, 8462.
(56) Ho, J.; Coote, M. L. *Theor. Chem. Acc.* **2010**, *125*, 3.
(57) Goering, H. L.; Briody, R. G.; Levy, J. F. *J. Am. Chem. Soc.* **1963**, *85*, 3059.
(58) Goering, H. L.; Levy, J. F. *J. Am. Chem. Soc.* **1964**, *86*, 120.
(59) Tsuji, Y.; Kim, S. H.; Saeki, Y.; Yatsugi, K.; Fujio, M.; Tsuno, Y. *Tetrahedron Lett.* **1995**, *36*, 1465.
(60) Allen, A. D.; Kanagasabapathy, V. M.; Tidwell, T. T. *J. Am. Chem. Soc.* **1985**, *107*, 4513.
(61) Bentley, T. W.; Schleyer, P. V. R. *Adv. Phys. Org. Chem.* **1977**, *14*, 1.
(62) Zhao, Y.; González-García, N.; Truhlar, D. G. *J. Phys. Chem. A* **2005**, *109*, 2012.
(63) Zhao, Y.; Truhlar, D. G. *J. Chem. Theory Comput.* **2011**, *7*, 669.
(64) Zhao, Y.; Truhlar, D. G. *Acc. Chem. Res.* **2008**, *41*, 157.
(65) Cramer, C. J.; Truhlar, D. G. *Chem. Rev.* **1999**, *99*, 2161.
(66) Tomasi, J.; Persico, M. *Chem. Rev.* **1994**, *94*, 2027.
(67) Tomasi, J.; Mennucci, B.; Cammi, R. *Chem. Rev.* **2005**, *105*, 2999.
(68) Stewart, J. J. P. *J. Mol. Model.* **2007**, *13*, 1173.
(69) Hostaš, J.; Řezáč, J.; Hobza, P. *Chem. Phys. Lett.* **2013**, *568*, 161.
(70) Mackerell, A. D., Jr. *J. Comput. Chem.* **2004**, *25*, 1584.
(71) Houk, K. N.; Rondan, N. G. *J. Am. Chem. Soc.* **1984**, *106*, 4294.
(72) Finn, M.; Friedline, R.; Suleman, N. K.; Wohl, C. J.; Tanko, J. M. *J. Am. Chem. Soc.* **2004**, *126*, 7578.
(73) Moss, R. A.; Wang, L.; Zhang, M.; Skalit, C.; Krogh-Jespersen, K. *J. Am. Chem. Soc.* **2008**, *130*, 5364.
(74) Truhlar, D. G.; Garrett, B. C. *Annu. Rev. Phys. Chem.* **1984**, *35*, 159.
(75) Lynch, B. J.; Truhlar, D. G. *J. Phys. Chem. A* **2001**, *105*, 2936.
(76) Zhao, Y.; Truhlar, D. G. *J. Phys. Chem. A* **2005**, *109*, 5656.
(77) Kluger, R.; Howe, G. W.; Mundle, S. O. C. *Adv. Phys. Org. Chem.* **2013**, *47*, 85.
(78) Mundle, S. O. C.; Rathgeber, S.; Lacrampe-Couloume, G.; Lollar, B. S.; Kluger, R. *J. Am. Chem. Soc.* **2009**, *131*, 11638.
(79) Kluger, R.; Mundle, S. O. C. *Adv. Phys. Org. Chem.* **2010**, *44*, 357.
(80) Bell, R. P.; Clunie, J. C. *Trans. Faraday Soc.* **1952**, *48*, 439.
(81) Bell, R. P. *Adv. Phys. Org. Chem.* **1966**, *4*, 1.
(82) Kurz, J. L. *J. Am. Chem. Soc.* **1967**, *89*, 3524.
(83) Kurz, J. L.; Coburn, J. I. *J. Am. Chem. Soc.* **1967**, *89*, 3528.
(84) Greenzaid, R.; Luz, Z.; Samuel, D. *J. Am. Chem. Soc.* **1967**, *89*, 749.
(85) Greenzaid, R.; Luz, Z.; Samuel, D. *J. Am. Chem. Soc.* **1967**, *89*, 756.
(86) Guthrie, J. P.; Cullimore, P. A. *Can. J. Chem.* **1980**, *58*, 1281.
(87) Guthrie, J. P.; Pitchko, V. *J. Am. Chem. Soc.* **2000**, *122*, 5520.
(88) Kurz, J. L.; Wexler, D. N. *J. Am. Chem. Soc.* **1975**, *97*, 2255.
(89) Llewellyn, D. R.; O'Connor, C. *J. Chem. Soc.* **1964**, 4400.
(90) Llewellyn, D. R.; O'Connor, C. *J. Chem. Soc.* **1964**, 545.
(91) O'Connor, C.; LLewellyn, D. R. *J. Chem. Soc.* **1965**, 2669.
(92) O'Connor, C.; LLewellyn, D. R. *J. Chem. Soc.* **1965**, 2197.
(93) Guthrie, J. P. *J. Phys. Chem. B* **2009**, *113*, 4501.
(94) Marenich, A. V.; Cramer, C. J.; Truhlar, D. G. *J. Phys. Chem. B* **2009**, *113*, 4538.
(95) Brown, T. N.; Mora-Diez, N. *J. Phys. Chem. B* **2006**, *110*, 9270.
(96) Gómez-Bombarelli, R.; González-Pérez, M.; Pérez-Prior, M. T.; Calle, E.; Casado, J. *J. Org. Chem.* **2009**, *74*, 4943.
(97) Takano, Y.; Houk, K. N. *J. Chem. Theory Comput.* **2005**, *1*, 70.
(98) Cossi, M.; Barone, V.; Cammi, R.; Tomasi, J. *Chem. Phys. Lett.* **1996**, *255*, 327.
(99) Shokri, A.; Abedin, A.; Fattahi, A.; Kass, S. R. *J. Am. Chem. Soc.* **2012**, *134*, 10646.
(100) Namazian, M.; Zakery, M.; Noorbala, M. R.; Coote, M. L. *Chem. Phys. Lett.* **2008**, *451*, 163.
(101) Namazian, M.; Heidary, H. *THEOCHEM* **2003**, *620*, 257.
(102) Guthrie, J. P. *Can. J. Chem.* **1999**, *77*, 934.
(103) Bernasconi, C. F. *Acc. Chem. Res.* **1992**, *25*, 9.
(104) Bernasconi, C. F. *Adv. Phys. Org. Chem.* **2010**, *44*, 223.
(105) Sauers, C. K.; Jencks, W. P.; Groh, S. *J. Am. Chem. Soc.* **1975**, *97*, 5546.
(106) Polovnikova, E. S.; McLeish, M. J.; Sergienko, E. A.; Burgner, J. T.; Anderson, N. L.; Bera, A. K.; Jordan, F. J.; Kenyon, G. L.; Hasson, M. S. *Biochemistry* **2003**, *42*, 1820.
(107) Brandt, G. S.; Kneen, M. M.; Petsko, G. A.; Ringe, D.; McLeish, M. J. *J. Am. Chem. Soc.* **2010**, *132*, 438.
(108) Kluger, R.; Tittmann, K. *Chem. Rev.* **2008**, *108*, 1797.
(109) Kluger, R.; Rathgeber, S. *FEBS J.* **2008**, *275*, 6089.
(110) Vardi-Kilshtain, A.; Doron, D.; Major, D. T. *Biochemistry* **2013**, *52*, 4382.
(111) Lewis, C. A.; Wolfenden, R. *Biochemistry* **2007**, *46*, 13331.
(112) Lewis, C. A. J.; Wolfenden, R. *Proc. Natl. Acad. Sci. U.S.A.* **2008**, *105*, 17328.
(113) Wolfenden, R. *Annu. Rev. Biochem.* **2011**, *80*, 645.
(114) Wolfenden, R.; Lewis, C. A., Jr.; Yuan, Y. *J. Am. Chem. Soc.* **2011**, *133*, 5683.
(115) Taylor, S. D.; Kluger, R. *J. Am. Chem. Soc.* **1993**, *115*, 867.